Article:
von der Heydt, Alice C and McLeish, Tom C B orcid.org/0000-0002-2025-0299 (2019) How proteins' negative cooperativity emerges from entropic optimisation of versatile collective fluctuations. The Journal of Chemical Physics. 215101. ISSN 1089-7690

https://doi.org/10.1063/1.5123741

How proteins' negative cooperativity emerges from entropic optimisation of versatile collective fluctuations

Alice von der Heydt[1, a)] and Tom C. B. McLeish[2]
[1)] *Department of Physics, University of York, Heslington, York, YO10 5DD, UK*
[2)] *Department of Physics & Centre for Medieval Studies, Humanities Research Centre, University of York, Heslington, York, YO10 5DD, UK*

(Dated: 17 October 2019)

The fact that allostery, a non-local signalling between distant binding sites, can arise mainly from the entropy balance of collective thermal modes, without conformational change, is by now well known. However, the propensity to generate negative cooperativity is still unclear. Starting from an elastic-network picture of small protein complexes, in which effector binding is modelled by locally altering interaction strengths in lieu of adding a node-spring pair, we elucidate mechanisms particularly for such negative cooperativity. The approach via a few coupled harmonic oscillators with internal elastic strengths, allows to trace individual eigenmodes, their frequencies, and their statistical weights, through successive bindings. We find that alteration of the oscillators' *couplings* is paramount to covering both signs of allostery. Binding-modified couplings create a rich set of eigenmodes individually for each binding state, modes unaccessible to an ensemble of non-interacting units. The associated shifts of collective-mode frequencies, non-uniform with respect to modes and binding states, result in an enhanced optimisability, reflected by a subtle phase map of allosteric behaviours.

I. INTRODUCTION

Regulation of activity via intra-protein, non-local signalling, called allosteric communication, is vital for many proteins to perform their functions[1–3]. For these allosteric proteins, binding events separated in space (and time) communicate remotely: binding one ligand either favours or inhibits the binding of a second, often identical one, at a site distant across the protein. Inhibition, or negative cooperativity, is essential in gene transcription, exemplified by the Catabolite Activator Protein of *Escherichia coli*[4,5], a transcription factor of the CRP/FNR family. Anti-cooperativity or negative allostery are common alternative terms. However, most basic models of allosteric regulation fail to capture negative cooperativity, which requires, *inter alia*, an enhanced sensitivity to ligand concentrations over a large range.

Whilst the term 'allostery' had been coined upon discovering binding-site cooperativity enabled by structural changes of proteins[1,6], alternative routes to allostery via modifications of statistically significant, collective modes of structurally mostly unaltered proteins[7] are by now well established[8–12]. To quantify this entropy-driven allostery, methods within the class of elastic network models (ENM), covering a spectrum of levels of coarse-graining, have proved successful[5,13–16]. In these protein models, treatment of generic interactions in linear response or harmonic approximation provides many advantages, yet restrictions as well: the eigenspectrum of thermal motion is readily accessible. Low-frequency global modes compatible with linear response, consistently dominate the predicted motion via large Boltzmann weights in the classical partition function. Yet this approach fails to account for contributions from dynamical constraints on the omitted finer-grained, *e.g.*, side-chain, structures[17,18].

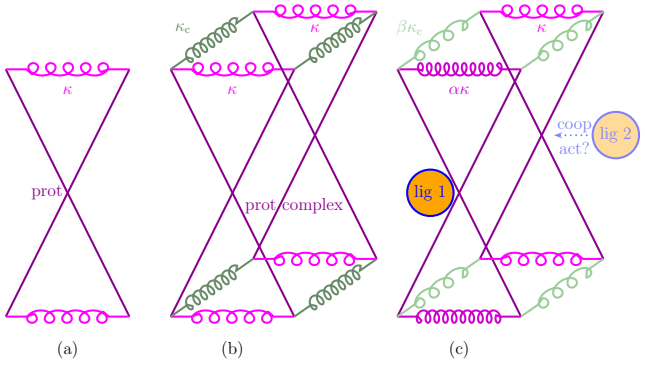

FIG. 1. (a) Protein or protomer represented by a scissor-shaped oscillator; (b) two coupled units; (c) binding at one modelled by local interaction-strength alterations.

To analyse a representative class of ENMs with transparent eigensystems that result in negative cooperativity, we focus on small rings of elastically coupled oscillators, each additionally possessing an internal elastic mode. Without loss of generality, we may depict each oscillator as scissor-shaped with a spring at each end, cf., Fig. 1, which establishes ties to the idea of an 'allosteron'[11,19,20], originally designed as a single unit to exemplify positive allostery. Building a model from the nodes' internal elastic structure in this way, avoids zero-energy modes of global translation and rotation usually predicted as an artefact of elastic network theory. In fact, this model can be perceived as a suitably coarse-grained ENM. Still, the emergence of distinctively collective modes and a non-uniform evolution of eigenvalues and -modes in response to binding, is enabled by the coupling alone. We recall that non-interacting elastic

[a)] Electronic mail: alice.vonderheydt@york.ac.uk

units whose internal strengths are thought to be altered in equal steps, can capture positive allostery only[11]. This follows from the free energies' logarithmic dependence on isolated mode strengths. Hence, any form of this model would be too restricted for the purpose of studying negative cooperativity.

Harmonic-oscillator rings with one-dimensional couplings may appear oversimplified to address allostery. With a minimal two-parameter binding model, however, these rings possess all requirements for non-trivial allosteric behaviour. As regards modelling of protein networks, even $1D$ springs faithfully map the connectivity, *i.e.*, interacting pairs and degrees of nodes — amino acids, protomers, or proteins —, depending on the coarse-graining. Given the accessibility of individual eigenmodes and associated -values, the impact of collective modes' interplay can be scrutinised, beyond mere numerical scanning of free-energy maps. Rings with their intrinsically stable topology are ubiquitous as both oligomeric proteins and complexes which involve several proteins, e.g., chaperones[21,22]. Haemoglobin, a hetero-tetramer ring, binds oxygen cooperatively[23,24]. Faces of polyhedral viral capsids are further prominent examples of rings, with highly symmetric inter-ring coupling[25,26]. Due to their periodic boundaries and symmetries, small rings may capture some of the salient intrinsic features of assemblies with more degrees of freedom as well. Whilst negative cooperativity has been found *inter alia* for ENM dimers, trimer and tetramer rings with binding-modified couplings[20,27], the aim here is to detail the *mechanism* for one workable and representative case.

This paper is organised as follows. The model is introduced in Section II, including definitions relating to elastic matrices and allosteric free energies. Section III is dedicated to the derivation and detailed analysis of eigensystem changes and their impact on cooperativity for the case of trimer rings, with a focus on those parameter sets which result in negative cooperative binding. The subset of pure coupling-strength alterations, a model instructive by its minimal parameter set sufficient to map both signs of allostery, is discussed in Subsec. III C. We summarise in Section IV, and show potential future paths along these lines.

II. MODEL

A. Coupled harmonic oscillators with binding-modified interaction strengths

We model protein complexes with effector binding by coupled harmonic oscillators, and the binding of a ligand as a local alteration of interaction strengths, in lieu of adding an oscillator-spring pair. Each oscillator is assumed to possess an internal elastic mode, whose strength may be altered by binding, independently of the strength alteration of adjacent couplings. The following set of properties proves to be sufficient to capture and display a mechanism for both signs of allostery:

- Internal elastic mode of strength κ, may represent protein's or protomer's 'breathing' mode
- Positive [in-phase] interaction of ≥ 2 oscillators, within harmonic approximation, via elastic coupling mode of strength κ_{c}
- Binding at one oscillator's site changes mode strengths locally, by the factor α for the internal, respectively, β for the adjacent coupling, modes

Depending on the desired level of coarse-graining, each oscillator may resemble a protein multimer, a single protein, or, maybe most intuitively, a protein's subunit, *e.g.*, a helix dimer of scissor shape. However, the scissor shape constitutes neither a constraint nor a completely faithful picture, but one possible geometric interpretation of the mathematical structure of positive harmonic coupling. The parameters which define the model of coupled oscillators with binding sites are summarised in Fig. 1.

B. Elastic energies

We go on to sketch the statistical-mechanical path to allosteric free energies by means of the basic dimer model represented in Fig. 1. First, the positive coupling of two oscillators, in linear response, results in the elastic part of the Hamiltonian (without momenta)

$$\mathcal{H}^{(0)} = \frac{1}{2}(x_1, x_2) H^{(0)} (x_1, x_2)^{\dagger}, \tag{1}$$

a quadratic form in terms of the amplitudes x_1, x_2, with the elastic matrix or Hessian

$$H^{(0)} = \begin{pmatrix} \kappa + \kappa_{\mathrm{c}} & -\kappa_{\mathrm{c}} \\ -\kappa_{\mathrm{c}} & \kappa + \kappa_{\mathrm{c}} \end{pmatrix} \tag{2}$$

In general, the elastic matrix encodes the coupled pairs, or the network's topology, along with relative interaction strengths. With regards to binding, $H^{(0)}$ is the elastic matrix of the unbound [apo] state.

Second, we apply the local modification of interaction strengths induced by ligand binding. To facilitate transparency in matrix calculations later, we switch to dimensionless elastic matrices in units of the internal mode strength κ, introducing the ratio $K_{\mathrm{c}} := \kappa_{\mathrm{c}}/\kappa$ of coupling to internal mode strength. The dimensionless elastic matrix of the singly bound state reads

$$\hat{H}^{(1)} = \begin{pmatrix} \alpha + \beta K_{\mathrm{c}} & -\beta K_{\mathrm{c}} \\ -\beta K_{\mathrm{c}} & 1 + \beta K_{\mathrm{c}} \end{pmatrix} \tag{3}$$

Herein, the parameter α quantifies the factor by which the internal-mode strength is modified upon binding, and β is the factor by which the strengths of adjacent couplings are modified. Finally, the completely bound [holo] state, with respect to ligands, features the elastic matrix

$$\hat{H}^{(2)} = \begin{pmatrix} \alpha + \beta^2 K_{\mathrm{c}} & -\beta^2 K_{\mathrm{c}} \\ -\beta^2 K_{\mathrm{c}} & \alpha + \beta^2 K_{\mathrm{c}} \end{pmatrix} \tag{4}$$

By construction, the eigenvalues of a dimensionless elastic matrix give the squared frequencies, in units of κ, of the respective eigenmodes. It may be worthwhile to recall that, to comply with linear response, only modes of reasonably small eigenfrequencies contribute to the spectrum of fluctuations relevant for entropy-driven allostery. Also, in practice, protein modes will be overdamped, which, however, does not affect their amplitudes from the point of view of statistical mechanics.

C. Allosteric free energies

Allosteric free energies quantify the difference of free energies of binding of successive events; free energies of binding in turn measure changes of free energy upon binding. Via computing the classical partition functions from the determinants of the respective states elastic matrices, the thermal-fluctuation or entropic free energy of binding for one site bound is obtained as

$$\frac{\Delta F^{(1)}}{k_{\mathrm{B}}T} = \frac{1}{2}\log\frac{\det\hat{H}^{(1)}}{\det\hat{H}^{(0)}} \tag{5}$$

The free energy of binding at two sites, now relative to the singly bound state, is, analogously,

$$\frac{\Delta F^{(2)}}{k_{\mathrm{B}}T} = \frac{1}{2}\log\frac{\det\hat{H}^{(2)}}{\det\hat{H}^{(1)}} \tag{6}$$

With reference to these three states, the allosteric free energy that characterises the cooperativity of a second binding, conditional on a first binding, is

$$\begin{aligned}\frac{\Delta\Delta F^{(2,1)}}{k_{\mathrm{B}}T} &:= \frac{\Delta F^{(2)} - \Delta F^{(1)}}{k_{\mathrm{B}}T} \\ &= \frac{1}{2}\log\frac{\det\hat{H}^{(2)}\det\hat{H}^{(0)}}{(\det\hat{H}^{(1)})^2}\end{aligned} \tag{7}$$

This definition amounts to a discrete second-order derivative, and so calls for cooperativity to be evaluated for exactly three states of effector-binding. Hence, in the case of complexes with more than two binding sites, the states for which cooperativity is analysed must be specified. Whenever individual eigenmodes are accessible and identifiable with their eigenvalues throughout all binding states, as for small rings, this expression can be recast to display each mode's contribution:

$$\frac{\Delta\Delta F^{(2,1)}}{k_{\mathrm{B}}T} = \frac{1}{2}\sum_i \log\frac{\lambda_i^{(2)}\lambda_i^{(0)}}{\lambda_i^{(1)}\lambda_i^{(1)}} \tag{8}$$

(i indexes linearly independent modes). Values of $\Delta\Delta F^{(2,1)} > 0$ indicate the free energy of binding, $\Delta F^{(2)}$, involved in the transition from one to two bound sites, to be larger than $\Delta F^{(1)}$, from zero to one; this amounts to negative cooperativity of the two binding events.

D. Limitations of a single-oscillator model

Due to the free energy's logarithmic dependence on (effective) mode strengths, models which employ two equal consecutive strength alterations of isolated or statically coupled units fail to capture negative cooperativity. The

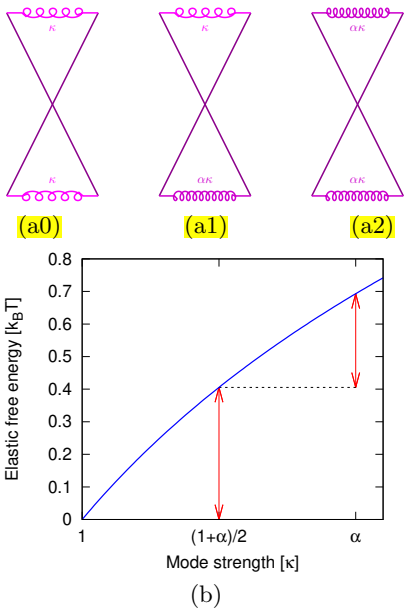

FIG. 2. (a) Two-step internal-strength modification of a single (uncoupled) elastic unit —(a0) no, (a1) one binding; (a2) two bindings— gives rise to (b) positive cooperativity, $\Delta\Delta F^{(2,1)} < 0$, only.

corresponding mechanism for a single 'allosteron' — two springs coupled rigidly; a single degree of freedom — is illustrated in Fig. 2. Independently of the sign of the first free energy of binding, $\Delta F^{(1)}$ (indicated by one of the vertical arrows in the lower panel of Fig. 2), the second, $\Delta F^{(2)}$ (indicated by the other arrow), will be either a smaller increase or a larger decrease of free energy.

E. Fluctuation allostery of a dimer with binding-modified interaction strengths

For a first idea of coupled oscillators' complex allosteric landscape, the dimer with two binding sites, cf., Fig. 1 and Eqs. (2) to (4), proves an instructive case. Evaluation of the allosteric free energy as a function of the binding-modifiers α and β results in the map shown in Fig. 3. Negative cooperative binding, indicated by positive values of $\Delta\Delta F^{(2,1)}$, is found in an extended parameter region for locally (binding-site) softened couplings, $\beta < 1$, for both signs of the internal-strength factor α. Perhaps surprisingly, another region of negative cooperativity opens from the point $\alpha = 1$, $\beta = 1$ towards $\beta > 1$.

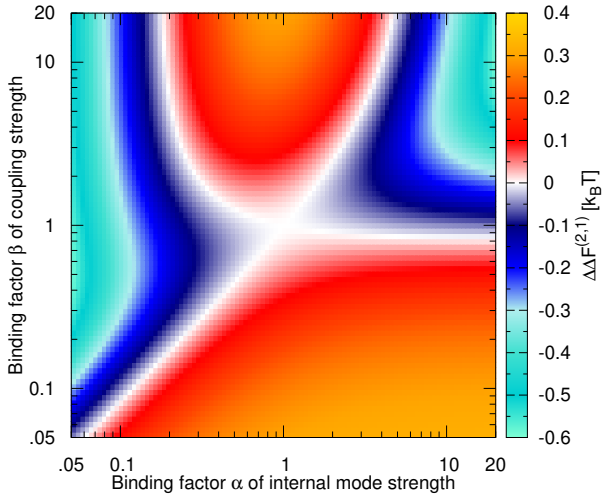

FIG. 3. Allosteric free energy $\Delta\Delta F^{(2,1)}(\alpha,\beta)$ of a dimer, at an initial coupling-to-internal strength ratio $K_c = 0.5$.

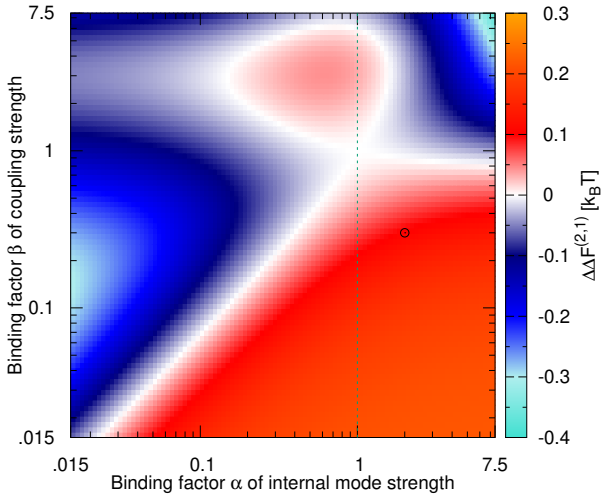

FIG. 4. Allosteric free energy $\Delta\Delta F^{(2,1)}(\alpha,\beta)$ of a trimer ring, at an initial coupling-to-internal strength ratio $K_c = 0.5$. The circle marks the modifier pair (α,β) discussed in detail in Sec. III B, the dashed line the case analysed in Sec. III C.

III. RESULTS: NEGATIVE COOPERATIVITY

Using the coarse-grained ENM with coupling modification introduced above, we go on to highlight how negative cooperativity arises. Given the uniformly positive cooperativity of the single-mode system, for even slightly more complex multi-mode networks, the detailed changes of the eigenspace are significant. The chosen class of small networks is minimal in regard to capturing negative cooperativity, in that the mechanism delivers a non-trivial landscape of allostery, yet remains sufficiently transparent to reveal its underlying structure.

A. Map of fluctuation allostery for trimer rings

Before continuing to the mode-specific analysis, a global map of the allosteric free energy $\Delta\Delta F^{(2,1)}$ from Eq. (7), of a representative trimer ring, in Fig. 4, allows us to identify the parameter region relevant to negative cooperativity. Here, the three states chosen to evaluate allosteric behaviour according to Eq. (7), are the apo state, i.e., without ligands bound, the singly bound, and the doubly bound state. That the small ENM features at least one 'inactive' site, still essential in supporting the collective modes relevant for fluctuation allostery, may aide the focus on the mechanism for a reasonably general case. The corresponding allosteric free energy according to Eqs. (7) or (8), as a function of α, β, K_c, is given in Appendix B. In Fig. 4, negative cooperativity, indicated by positive values of $\Delta\Delta F^{(2,1)}$, occurs mainly for locally binding-softened couplings, $\beta < 1$, again for both signs of α. However, weakly negative cooperativity also exists in a confined, closed region of strengthened couplings, $\beta > 1$, for values of α of the order of 1.

B. Eigensystems of trimer rings

We begin the analysis of how negative cooperativity emerges from the rings' eigensystems, by identifying the eigenmodes and -values of the unbound [apo] state of a trimer ring; see Fig. 5 for an illustration of this first case. In what follows, miniature spring-bound scissors (purple) inside circles at the triangles' corners represent the oscillators, while springs (green) along the triangles edges represent the couplings. A smaller number of coils and a brighter green will indicate softening of a coupling spring. All descriptions of amplitude vectors implicitly assume fluctuation modes to be overdamped, thus refer to the respective modes' adiabatic continuations.

The smallest eigenvalue, $\lambda_1^{(0)} = 1$, belongs to the adiabatic continuation of a mode labelled 1, in which all three oscillators' fluctuations have equal amplitudes and signs, shown by [red] arrows in the top panel of Fig. 5. (For Gaussian networks without internal degrees of freedom, the analogous uniform-translation mode has zero frequency.) In the unbound state, a single larger eigenvalue is shared or degenerate by two different eigenmodes, visualised in the bottom panel of Fig. 5: The mode depicted by dotted [orange] arrows, labelled 2 in the following, has two equal entries; the remaining entry has the opposite sign and twice the amplitude. In the mode depicted by solid [blue] arrows, labelled 3 in what follows, two oscillators fluctuate out-of-phase with equal amplitudes, the third is at rest. Mode 3 will be seen to be invariant, except for the order of its entries, under any binding-induced modification of parameters. We pause to observe that, due to the symmetry of the unbound state, each of its eigenvectors is invariant under label permutations.

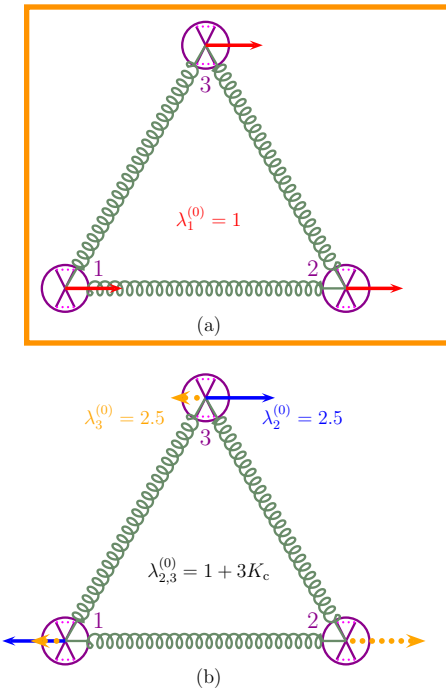

FIG. 5. Eigenmodes and -values of a trimer ring in the (unbound) state without ligand binding; (a) mode 1, (b) modes 2 and 3. Numerical eigenvalues $\lambda_{2,3}^{(0)}$ displayed for $K_c = 0.5$.

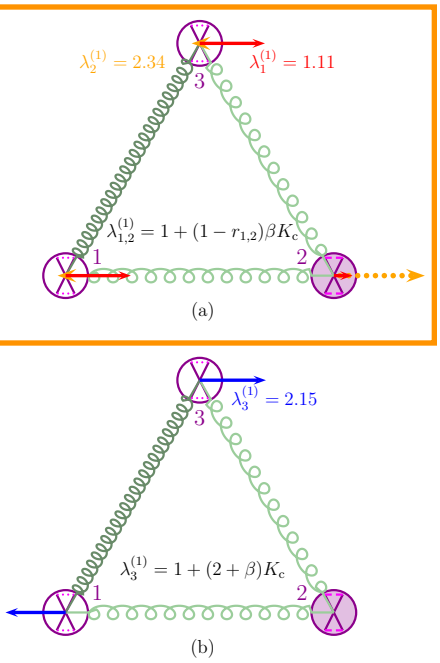

FIG. 6. Eigenmodes and -values in the singly bound state; (a) modes 1 and 2, (b) mode 3; numerical values for $K_c = 0.5$, $\alpha = 2$, $\beta = 0.3$.

Moving on to the singly bound state, we recall that one oscillator's internal strength is altered by a factor α, here $\alpha = 2$, the strength of the adjacent coupling springs by a factor β, here $\beta = 0.3$. The situation is shown in Fig. 6, with the bound site displayed as a filled circle, for $\alpha > 1$, $\beta < 1$, the parameter set marked by a small open circle in Fig. 4. (Explicit expressions for the eigenvalues and -modes of all three binding states, in terms of α, β, and K_c, can be found in Appendix A.) In fact, the adapted eigenmodes' shapes for any parameter set can be inferred from symmetry considerations: Mode 1, with all amplitudes in phase and of equal signs, now has a single amplitude differing in magnitude from the two remaining equal ones, located at the bound site, which breaks the (complete) symmetry of the apo state. This single amplitude is markedly smaller than the two remaining ones. Mode 2, by eigenvalue conjugate to 1, maintains the structure of two equal entries, and one of opposite sign and different amplitude. The last is now pinned at the bound site via the mentioned local symmetry reduction. Similarly, the site at rest in the anti-phase mode 3, whose vector entries are invariant under the modifiers α, β, is also confined to the bound site. The zero amplitude of the only oscillator whose breathing mode is changed by α, implies that the respective eigenvalue $\lambda_3^{(1)}$ is affected by the coupling-strength modifier β only.

The doubly bound state is visualised in Fig. 7, for the same set of $\alpha > 1$, $\beta < 1$ as in Fig. 6. The amplitude configuration of the in-phase mode 1 changes considerably once more, in that now only one larger amplitude is

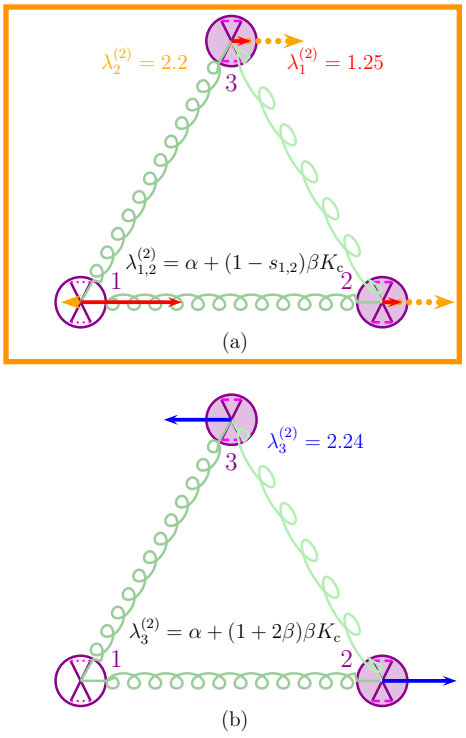

FIG. 7. Eigenmodes and -values in the doubly bound state; (a) modes 1 and 2, (b) mode 3; numerical values for $K_c = 0.5$, $\alpha = 2$, $\beta = 0.3$.

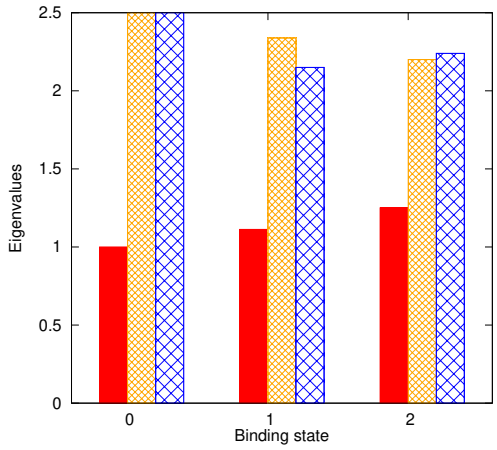

FIG. 8. Eigenvalues for $K_c = 0.5$, $\alpha = 2$, $\beta = 0.3$. Modes in each stack: left, solid (red) 1; centre (yellow) 2; right, hatched (blue) 3.

present, localised at the unbound, non-strengthened site. This is the pinning site also for the single anti-phase entry of mode 2, however, of tiny amplitude compared to the large equal amplitudes at the bound sites. Mode 3, with its vector entries independent of binding state and modifiers, is accommodated by restricting the single unbound site to be at rest.

The evolution of the eigenvalues under the binding transitions is summarised in Fig. 8. For the parameters discussed, eigenvalues λ_2 and λ_3 first differentiate, then exchange order in a list according to size, almost regaining parity in the doubly bound state. On the first binding, both λ_2 and λ_3 decrease relative to their values in the unbound state. Because for mode 2, the singled-out amplitude pinned at the internally strengthened, bound site is large, the decrease in λ_2 is less than that in λ_3. Through the second binding, λ_2 continues to decrease, however, moderately. In contrast, λ_3 increases slightly again relative to $\lambda_3^{(1)}$, due to the two nonzero entries of mode 2 at the stiffened sites, additionally loading the two stronger, *i.e.*, only partially weakened couplings.

The maps of mode-specific contributions according to Eq. 8 to the allosteric free energy $\Delta\Delta F^{(2,1)}(\alpha, \beta)$, in Fig. 9, underline how non-uniformly the modes and their impacts onto $\Delta\Delta F^{(2,1)}$ transform under binding. Whereas mode 1's contribution to allostery is globally small, modes 2 and 3 have nearly opposite impacts in regard to signs of allostery. In particular, for the parameter set chosen, marked by a circle toward the bottom right border of the map, mode 3 is clearly the mode decisive for the sign of allostery, as readily seen from the order of eigenvalues in Fig. 8.

A preliminary conclusion from this example-supported discussion is that optimal adaption and localisation of eigenmodes minimises the free energy (change) of binding, $\Delta F^{(1)}$, at the first event already. An essential part of this optimisation is the pinning of the entropically 'costly'

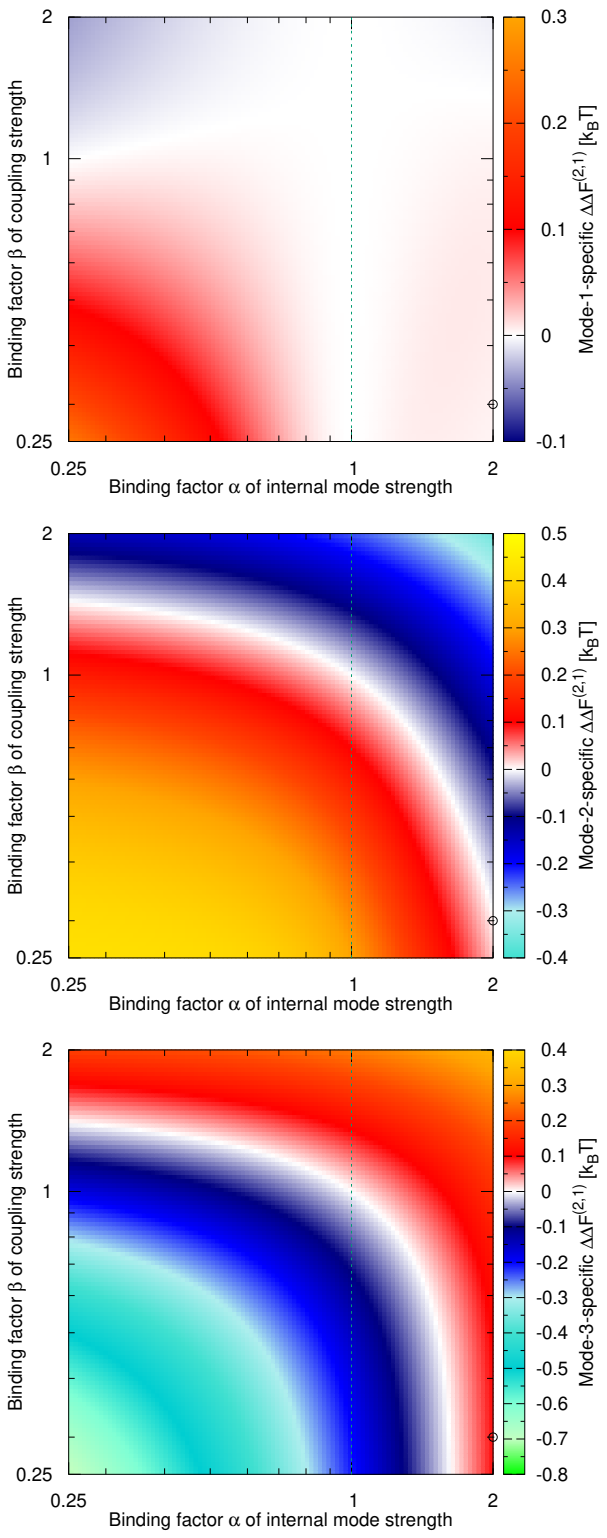

FIG. 9. Mode-specific contributions to allosteric free energy $\Delta\Delta F^{(2,1)}(\alpha, \beta)$; $K_c = 0.5$ as in Fig. 4.Note the zoom into a smaller parameter region compared to that of Fig. 4.

anti-phase mode 3 such that the first bound, here internally stiffened, site is confined to remain at rest. Similarly, the second mode of comparatively high frequency (2 in our labelling) adapts to the first binding by localising at the bound site the single amplitude out of phase with the two others, thus loading the weakened couplings only. For the second binding, with another stiffened site constraining further the thermally accessible states, this entropic optimisation of the modes is seen to work less effectively. Negative allostery is seen to be brought about by different modes' eigenfrequencies changing with marked inhomogeneity through binding. Finally, a coupled-oscillator model's potential for re-ordering of modes according to the magnitude of associated eigenvalues might be a vital ingredient of entropy-driven allostery of both signs in general. This contrasts with the scenario for a single elastic degree of freedom, allowing for two equal increments of a sole effective mode strength only, as illustrated in Fig. 2.

C. Coupling-strength alteration only

Within the model introduced, negative allostery can be realised even without modifying the internal mode strength under ligand binding, *i.e.*, on the vertical line $\alpha = 1$ in the map of Fig. 4. One reason not to have selected such a system for visualisation in the first place is that for $\alpha = 1$, all eigenmodes shown in Fig. 5 remain invariant under binding, up to permutation or localisation of entries, as we explain in the following.

Due to the binding protocol affecting the coupling only, the symmetry with respect to the three oscillators' internal strengths is conserved, leaving all modes' amplitude ratios invariant. The elastic matrix $\hat{H}$ remains a linear combination of the identity matrix $\mathbb{1}$ (recall all oscillators possess identical internal strengths) and a matrix C of connectivity or Laplacian form,

$$H = \mathbb{1} + K_{\mathrm{c}} C, \tag{9}$$

so that $\hat{H}$ and C share a common set of eigenvectors in all three binding states. For the chosen deterministic rings, the matrix C encodes harmonic interactions between fixed pairs, independently of the order or the degree of altering the strength of these interactions. Also, the in-phase mode 1 belongs to the kernel of *all* Laplacian matrices (whose rows and columns sum to zero), thereby attaining a nonzero eigenfrequency purely from the internal elastic strengths, or the identity matrix, the latter constant for all three states. In effect, not only is the eigenfrequency belonging to mode 1 invariant under pure coupling-strength alterations, but also mode 1 itself. For a three-dimensional (orthogonal) eigensystem of symmetric matrices, this restricts also the remaining modes 2 and 3 to be invariant, up to index permutations.

However, along the statistical-mechanics lines of analysing negative allostery, this case is worthwhile studying, as an extreme case of the mentioned disparity of the eigenfrequencies' evolution. In Table I, we summarise the eigenvalues for the general case of $\alpha = 1$, whereas the evolution for a specific set of coupling parameters (K_{c}, β) is displayed in Fig. 10. As hinted at above, mode 1 does not load any couplings, irrespectively of their (modified) strengths, therefore, eigenvalue λ_1 does not change at all under binding. The relevant coupling term of λ_2, associated with a mode of two equal entries, and one entry antiparallel, twice as large, is multiplied by the coupling modifier β in the first binding, however, sees no incremental change in the second binding. By inspection of Figs. 6 and 7, the relative motion of mode 2 is sensitive only to the same two, singly altered, couplings in both states. In contrast, the first binding changes the coupling term of λ_3, associated with anti-parallel motion of two allosterons, one at rest, only sub-linearly. The second binding, however, causes a multiplication of the entire coupling term by β, because in the holo state, the nonzero anti-parallel amplitudes are re-localised to load the softest coupling (Fig. 7).

Analysis of the allosteric free energy's sign in this case shows that anti-cooperative binding, or $\Delta\Delta F^{(2,1)} > 0$, occurs also for a range of $\beta > 1$, provided the initial coupling-to-internal strength ratio $K_{\mathrm{c}} < 2$. The exact condition for negative cooperativity reads as follows:

$$\beta < \frac{5K_{\mathrm{c}} + 2}{3K_{\mathrm{c}}^2} \quad (\beta \neq 1) \tag{10}$$

	apo$^{(0)}$	singly bound$^{(1)}$	holo$^{(2)}$
λ_1	1	1	1
λ_2	$1 + 3K_{\mathrm{c}}$	$1 + 3\beta K_{\mathrm{c}}$	$1 + 3\beta K_{\mathrm{c}}$
λ_3	$1 + 3K_{\mathrm{c}}$	$1 + (2 + \beta)K_{\mathrm{c}}$	$1 + (1 + 2\beta)\beta K_{\mathrm{c}}$

TABLE I. Binding-induced evolution of the eigenvalue spectrum for coupling-strength alteration only, $\alpha = 1$.

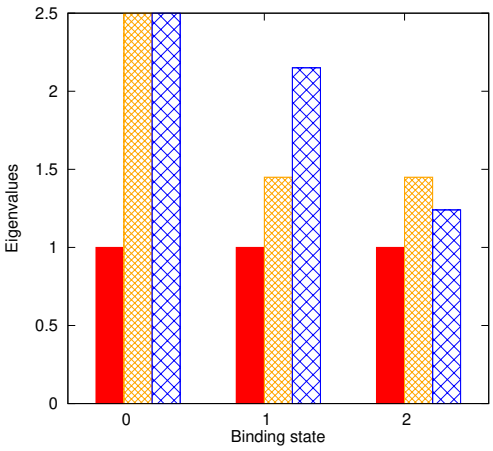

FIG. 10. Eigenvalues for $K_{\mathrm{c}} = 0.5$, $\alpha = 1$, $\beta = 0.3$. Modes in each stack: left, solid (red) 1; centre (yellow) 2; right, hatched (blue) 3.

1. Perturbation analysis

An alternative, perhaps more familiar, way of computing the (approximate) changes in eigenfrequencies under consecutive bindings, is provided by perturbation theory, routinely applied in quantum mechanics. By relative energy and size of a typical ligand, compared with protein scales, allosteric regulation is in fact of perturbative nature in most cases[28]. However, as for the chosen system, all frequency ratios can be computed exactly, we only sketch the approach here.

First, for the transition to the singly bound state, the perturbation Hamiltonian's matrix, with the parameter $\varepsilon := \beta - 1$, is

$$\Delta\hat{H}^{(1,0)} = \varepsilon K_\mathrm{c} \begin{pmatrix} 1 & -1 & 0 \\ -1 & 2 & -1 \\ 0 & -1 & 1 \end{pmatrix} \tag{11}$$

For unaltered internal strengths, also the perturbation matrices maintain the form of connectivity or Laplacian matrices. With the normalised eigenvectors, $\hat{\mathbf{v}}_i^{(0)}$, $i = 1, 2, 3$, of the reference (unbound) state according to Eqs. (A2a) to (A2c), we find

$$\Delta\lambda_1^{(1,0)} = \left\langle \hat{\mathbf{v}}_1^{(0)} | \Delta\hat{H}^{(1,0)} | \hat{\mathbf{v}}_1^{(0)} \right\rangle = 0 \tag{12a}$$

$$\Delta\lambda_2^{(1,0)} = \left\langle \hat{\mathbf{v}}_2^{(0)} | \Delta\hat{H}^{(1,0)} | \hat{\mathbf{v}}_2^{(0)} \right\rangle = 3\,\varepsilon K_\mathrm{c} \tag{12b}$$

$$\Delta\lambda_3^{(1,0)} = \left\langle \hat{\mathbf{v}}_3^{(0)} | \Delta\hat{H}^{(1,0)} | \hat{\mathbf{v}}_3^{(0)} \right\rangle = \varepsilon K_\mathrm{c} \tag{12c}$$

Note that for the coupling modifier $\beta = 0.3$, chosen for Fig. 10, the perturbation parameter $\varepsilon < 0$. For this perturbation linear in ε, the first-order perturbation analysis yields the exact changes, as expected, and confirmed by inspection of Table I. The magnitude of change in λ_2 is three times as large as that in λ_3.

The transition from the first to the second binding is encoded in the linear perturbation matrix

$$\Delta\hat{H}^{(2,1)} = \varepsilon K_\mathrm{c} \begin{pmatrix} 1 & 0 & -1 \\ 0 & 1 & -1 \\ -1 & -1 & 2 \end{pmatrix}, \tag{13}$$

A nonlinearity arises at sites 2 and 3, whose interaction is altered by factor β^2 due to the second binding at site 3, which follows the first binding at site 2. The first-order perturbation theory, however, predicts the following, inaccurate, changes in eigenvalues:

$$\Delta\lambda_1^{(2,1)} \approx \left\langle \hat{\mathbf{v}}_1^{(1)} | \Delta\hat{H}^{(2,1)} | \hat{\mathbf{v}}_1^{(1)} \right\rangle = 0 \tag{14a}$$

$$\Delta\lambda_2^{(2,1)} \approx \left\langle \hat{\mathbf{v}}_2^{(1)} | \Delta\hat{H}^{(2,1)} | \hat{\mathbf{v}}_2^{(1)} \right\rangle = \frac{3}{2}\varepsilon K_\mathrm{c} \tag{14b}$$

$$\Delta\lambda_3^{(2,1)} \approx \left\langle \hat{\mathbf{v}}_3^{(1)} | \Delta\hat{H}^{(2,1)} | \hat{\mathbf{v}}_3^{(1)} \right\rangle = \frac{3}{2}\varepsilon K_\mathrm{c}, \tag{14c}$$

particularly, erroneously, a change of λ_2 under the second binding. Despite this shortcoming of treating the transition from the singly to the doubly bound state perturbatively, the 'mode-coupling' pathway to negative allostery is still visible; after the first binding, modes 2 and 3 switch roles as concerns largest coupling to the binding — a path accessible to a coupled multi-mode model only.

IV. CONCLUSIONS

In this work, we have devised and analysed low-dimensional elastic network models (ENM) with local variation of harmonic interaction strengths to capture the mechanism of allosteric proteins' negative entropic cooperativity. Our main conclusion is that strength *variation of couplings* emanating from a site upon effector binding is essential for ENM with constant number of oscillators to map entropic cooperativity of both signs. While we had observed negative cooperativity in coupling-varied linear and ring ENM formed of 2–5 oscillators earlier[20], trimer rings have been chosen as an example set amenable to the detailed analysis considered inescapable. Original eigensystems distinctive of each binding state, found also in this simple example set, are accessible exclusively to a coupled system. Negative cooperativity arises entropically when the eigenfunction response to the variation of coupling strengths is tuned in a particular way. As a manifestation of this subtle tuning, modes of initially identical or similar eigenfrequency separate through the two bindings, and may even exchange positions in the order of their eigenfrequencies. In the class of low-dimensional, coupling-varied ENM whose cooperativity we looked into, the possibility of two consecutive alterations of the same coupling results in nonlinear effects. The last add to the complexity of the maps of cooperativity and potentially open up routes to negative cooperative binding not originally aimed at. However, hinting at requirements for negative cooperativity applicable to a larger class of protein ENM, a binding-induced sequence of coupling-strength alterations within the same 'chain' of sites might be a crucial ingredient.

In Sec. III B, we have seen in detail how modes of comparatively large frequency in the unbound state can be adjusted to the reduced symmetry of the singly bound state. Larger amplitudes are confined to internally softer sites, and/or load weaker couplings only, resulting in a decrease or minimal increase of free energy by the first binding. At the second binding, the mode optimisation towards entropy change minimisation turns out to be less effective, presumably due to the constraints imposed on the modes' symmetries and patterns already by the first event. For binding-induced internal stiffening and weakening of couplings, with respect to entropy maximisation, internal stiffening of another, so far unaffected site overcompensates the second (multiplicative) weakening of coupling strengths, which may affect springs modified already. If for the first event, free energy decreased, the second event can only accommodate a smaller reduction of free energy, or even effects a slight increase.

Although the results clearly suggest that binding-induced modification of coupling strengths is required for constant-spring-number ENM to map negative (in addition to positive) cooperativity, we had to stop short of isolating and proving minimally sufficient requirements. A rigorous proof along these lines will be the obvious follow-up to the present study To corroborate that, put slightly differently, networks with static coupling can map positive cooperativity only, more ENM amenable to mode analysis should be studied, or revisited. One of the next-simplest models are tetramer rings, providing additionally the chance to evaluate a holo state of non-adjacent sites[20]. Cooperativity in the assembly of networks of high symmetry, e.g., viral capsids[25], is worthwhile analysing by statistical mechanical tools for ENM as well. Another extension of this work relates to the coupling of modes in *dynamic* allostery[18], addressing the interplay of slow and fast modes due to, *e.g.*, side-chains.

ACKNOWLEDGMENTS

The authors gratefully acknowledge the funding of this project by the Engineering and Physical Sciences Research Council via grant number EP/N031431/1.

Appendix A: Eigensystems of trimer rings

For a quicker view on the modes' overall patterns, we provide orthogonal, but non-normalised eigenbases.

1. Unbound [apo] state

In analogy with the examples of elastic matrices presented in Subsec. II B, the elastic matrix of the unbound trimer ring reads

$$\hat{H}^{(0)} = \begin{pmatrix} 1+2K_\mathrm{c} & -K_\mathrm{c} & -K_\mathrm{c} \\ -K_\mathrm{c} & 1+2K_\mathrm{c} & -K_\mathrm{c} \\ -K_\mathrm{c} & -K_\mathrm{c} & 1+2K_\mathrm{c} \end{pmatrix}, \tag{A1}$$

Its eigenvalues and eigenvectors are

$$\lambda_1^{(0)} = 1 \qquad \mathbf{v}_1^{(0)} = \begin{pmatrix} 1 \\ 1 \\ 1 \end{pmatrix} \tag{A2a}$$

$$\lambda_{2,3}^{(0)} = 1+3K_\mathrm{c} \qquad \mathbf{v}_2^{(0)} = \begin{pmatrix} 1 \\ -2 \\ 1 \end{pmatrix} \tag{A2b}$$

$$\mathbf{v}_3^{(0)} = \begin{pmatrix} -1 \\ 0 \\ 1 \end{pmatrix} \tag{A2c}$$

2. Singly bound state

The elastic matrix of the state with one occupied binding site (labelled 2, without loss of generality),

$$\hat{H}^{(1)} = \begin{pmatrix} 1+(1+\beta)K_\mathrm{c} & -\beta K_\mathrm{c} & -K_\mathrm{c} \\ -\beta K_\mathrm{c} & \alpha+2\beta K_\mathrm{c} & -\beta K_\mathrm{c} \\ -K_\mathrm{c} & -\beta K_\mathrm{c} & 1+(1+\beta)K_\mathrm{c} \end{pmatrix}, \tag{A3}$$

features the eigenvalues and -vectors

$$\lambda_1^{(1)} = 1+(1-r_1)\beta K_\mathrm{c} \qquad \mathbf{v}_1^{(1)} = \begin{pmatrix} 1 \\ r_1 \\ 1 \end{pmatrix} \tag{A4}$$

$$\lambda_2^{(1)} = 1+(1-r_2)\beta K_\mathrm{c} \qquad \mathbf{v}_2^{(1)} = \begin{pmatrix} 1 \\ r_2 \\ 1 \end{pmatrix} \tag{A5}$$

with

$$r_{1,2} := f \pm \sqrt{2+f^2} \qquad r_2 = -\frac{2}{r_1} \tag{A6a}$$

$$f\left(\frac{\alpha-1}{\beta K_\mathrm{c}}\right) := -\frac{1}{2}\left(1+\frac{\alpha-1}{\beta K_\mathrm{c}}\right) \tag{A6b}$$

$$\lambda_3^{(1)} = 1+(2+\beta)K_\mathrm{c} \qquad \mathbf{v}_3^{(1)} = \begin{pmatrix} -1 \\ 0 \\ 1 \end{pmatrix} \tag{A7}$$

3. Doubly bound [holo] state

The elastic matrix of the state with two occupied binding sites (here, labelled 2 and 3),

$$\hat{H}^{(2)} = \begin{pmatrix} 1+2\beta K_\mathrm{c} & -\beta K_\mathrm{c} & -\beta K_\mathrm{c} \\ -\beta K_\mathrm{c} & \alpha+(1+\beta)\beta K_\mathrm{c} & -\beta^2 K_\mathrm{c} \\ -\beta K_\mathrm{c} & -\beta^2 K_\mathrm{c} & \alpha+(1+\beta)\beta K_\mathrm{c} \end{pmatrix}, \tag{A8}$$

has eigenvalues and -vectors as follows:

$$\lambda_1^{(2)} = \alpha+(1-s_1)\beta K_\mathrm{c} \qquad \mathbf{v}_1^{(2)} = \begin{pmatrix} s_1 \\ 1 \\ 1 \end{pmatrix} \tag{A9}$$

$$\lambda_2^{(2)} = \alpha+(1-s_2)\beta K_\mathrm{c} \qquad \mathbf{v}_2^{(2)} = \begin{pmatrix} s_2 \\ 1 \\ 1 \end{pmatrix} \tag{A10}$$

with

$$s_{1,2} := g \pm \sqrt{2+g^2} \tag{A11a}$$

$$g\left(\frac{\alpha-1}{\beta K_\mathrm{c}}\right) := -\frac{1}{2}\left(1-\frac{\alpha-1}{\beta K_\mathrm{c}}\right) \tag{A11b}$$

$$\lambda_3^{(2)} = \alpha + (1+2\beta)\beta K_\mathrm{c} \qquad \mathbf{v}_3^{(2)} = \begin{pmatrix} 0 \\ 1 \\ -1 \end{pmatrix} \tag{A12}$$

Appendix B: Allosteric free energy

The allosteric free energy according to the definition Eq. (8), evaluated for trimer rings and the parameter set α, β, K_c, takes the form

$$2\frac{\Delta\Delta F^{(2,1)}}{k_\mathrm{B}T} = \log\frac{\Big(\alpha+(1+2\alpha)\beta K_\mathrm{c}\Big)\,(1+3K_\mathrm{c})}{\Big(\alpha+(2+\alpha)\beta K_\mathrm{c}\Big)^2} + \log\frac{(1+3K_\mathrm{c})\,\Big(\alpha+(1+2\beta)\beta K_\mathrm{c}\Big)}{\Big(1+(2+\beta)K_\mathrm{c}\Big)^2} \tag{B1}$$

[1] J. Monod, J. Wyman, and J.-P. Changeux, "On the nature of allosteric transitions: a plausible model," J. Mol. Biol. **12**, 88–118 (1965).

[2] S. J. Wodak, E. Paci, N. V. Dokholyan, I. N. Berezovsky, A. Horovitz, *et al.*, "Allostery in Its Many Disguises: From Theory to Applications," Structure **27** (2019).

[3] E. Guarnera and I. N. Berezovsky, "Toward Comprehensive Allosteric Control over Protein Activity," Structure **27**, 866 (2019).

[4] N. Popovych, S. Sun, R. H. Ebright, and C. G. Kalodimos, "Dynamically driven protein allostery," Nat. Struct. Mol. Biol. **13**, 831 (2006).

[5] T. L. Rodgers, P. D. Townsend, D. Burnell, M. L. Jones, S. A. Richards, T. C. B. McLeish, E. Pohl, M. R. Wilson, and M. J. Cann, "Modulation of Global Low-Frequency Motions Underlies Allosteric Regulation: Demonstration in CRP/FNR Family Transcription Factors," PLoS Biol. **11**, e1001651 (2013).

[6] J.-P. Changeux and S. J. Edelstein, "Allosteric mechanisms of signal transduction," Science **308**, 1424–28 (2005).

[7] A. Cooper and D. T. F. Dryden, "Allostery without conformational change: a plausible model," Eur. Biophys. J. **11**, 103 (1984).

[8] B. Tidor and M. Karplus, "The contribution of vibrational entropy to molecular association. the dimerization of insulin." J. Mol. Biol. **238**, 405–14 (1994).

[9] M. K. Gilson, J. A. Given, B. L. Bush, and J. A. McCammon, "The statistical-thermodynamic basis for computation of binding affinities: a critical review." Biophys. J. **72**, 1047–69 (1997).

[10] R. J. Hawkins and T. C. B. McLeish, "Coarse-grained model of entropic allostery," Phys. Rev. Lett. **93**, 098104 (4pp) (2004).

[11] T. C. B. McLeish, T. L. Rodgers, and M. R. Wilson, "Allostery without conformation change: modelling protein dynamics at multiple scales," Phys. Biol. **10**, 056004 (9pp) (2013).

[12] R. Nussinov and C.-J. Tsai, "Allostery without a conformational change? Revisiting the paradigm," Curr. Op. Struct. Biol. **30**, 17–24 (2015).

[13] P. Durand, G. Trinquier, and Y. H. Sanejouand, "New approach for determining low-frequency normal-modes in macromolecules," Biopolymers **34**, 759–771 (1994).

[14] M. M. Tirion, "Large Amplitude Elastic Motions in Proteins from a Single-Parameter, Atomic Analysis," Phys. Rev. Lett. **77**, 1905 (4pp) (1996).

[15] I. Bahar, T. R. Lezon, A. Bakan, and I. H. Shrivastava, "Normal mode analysis of biomolecular structures: functional mechanisms of membrane proteins," Chem. Rev. **110**, 1463 (2010).

[16] T. C. B. McLeish, M. J. Cann, and T. L. Rodgers, "Dynamic Transmission of Protein Allostery without Structural Change: Spatial Pathways or Global Modes?" Biophys. J. **109**, 1240 (2015).

[17] R. J. Hawkins, *Coarse-grained models of dynamic allostery in proteins*, Ph.D. thesis, University of Leeds (2005).

[18] R. J. Hawkins and T. C. B. McLeish, "Coupling of Global and Local Vibrational Modes in Dynamic Allostery," Biophys. J. **91**, 2055 (2006).

[19] T. C. B. McLeish, "Slow Brownian fluctuations for allosteric signalling without structural change," in *Royal Society Discussion Meeting 'Allostery and Molecular Machines', London* (2017).

[20] T. C. B. McLeish, A. C. von der Heydt, and C. Schaefer, "The 'allosteron' model for entropic allostery of self-assembly," Phil. Trans. R. Soc. B **373**, 20170186 (2018).

[21] P. B. Sigler, Z. Xu, H. S. Rye, S. G. Burston, W. A. Fenton, and A. L. Horwich, "Structure and function in GroEL-mediated protein folding," Annu. Rev. Biochem. **67**, 581 (1998).

[22] W. Zheng, B. R. Brooks, and D. Thirumalai, "Allosteric Transitions in the Chaperonins groEL are Captured by a Dominant Normal Mode that is Most Robust to Sequence Variations," Biophys. J. **93**, 2289–2299 (2007).

[23] C. Ciaccio, A. Coletta, G. De Sanctis, S. Marini, and M. Coletta, "Cooperativity and Allostery in Haemoglobin Function," IUBMB Life **60**, 112–123 (2008).

[24] C. Bohr, K. Hasselbach, and A. Krogh, "Ueber einen in biologischer Beziehung wichtigen Einfluss, den die Kohlensäurespannung des Blutes auf dessen Sauerstoffbindung übt," Skand. Arch. Physiol. **15**, 401–412 (1904).

[25] A. Zlotnick, "To Build a Virus Capsid: An Equilibrium Model of the Self Assembly of Polyhedral Protein Complexes," J. Mol. Biol. **241**, 59 (1994).

[26] R. Twarock, "Mathematical virology: a novel approach to the structure and assembly of viruses," Phil. Trans. R. Soc. A **364**, 3357 (2006).

[27] H. Toncrova, *Coarse-grained models of biomolecule dynamics and allostery*, Ph.D. thesis, University of Leeds (2010).

[28] E. Guarnera and I. N. Berezovsky, "On the perturbation nature of allostery: sites, mutations, and signal modulation," Curr. Op. Struct. Biol. **56**, 18 (2019).